

Statistica Sinica Preprint No: SS-2022-0248

| | |
|---------------------------------|---|
| Title | Decoupling Systemic Risk into Endopathic and Exopathic Competing Risks Through Autoregressive Conditional Accelerated Fréchet Model |
| Manuscript ID | SS-2022-0248 |
| URL | http://www.stat.sinica.edu.tw/statistica/ |
| DOI | 10.5705/ss.202022.0248 |
| Complete List of Authors | Jingyu Ji, Deyuan Li and Zhengjun Zhang |
| Corresponding Authors | Deyuan Li |
| E-mails | deyuanli@fudan.edu.cn |

Decoupling Systemic Risk into Endopathic and Exopathic Competing Risks Through Autoregressive Conditional Accelerated Fréchet Model

Jingyu Ji^a, Deyuan Li^b, Zhengjun Zhang^{c,d,e}

^aCapital University of Economics and Business, ^bFudan University,

^cUniversity of Chinese Academy of Sciences, ^dChinese Academy of

^eUniversity of Wisconsin

Abstract: Identifying systemic risk patterns in geopolitical, economic, financial, environmental, transportation, epidemiological systems and their impacts is the key to risk management. This paper proposes a new nonlinear time series model: autoregressive conditional accelerated Fréchet (AcAF) model and introduces two

Corresponding authors: Deyuan Li, Department of Statistics and Data Science, School of Management, Fudan University, Shanghai, China. E-mail: deyuanli@fudan.edu.cn. Zhengjun Zhang, School of Economics and Management, and MOE Social Science Laboratory of Digital Economic Forecasts and Policy Simulation, University of Chinese Academy of Sciences, Beijing, China; Center for Forecasting Sciences, Chinese Academy of Sciences, Beijing, China; Department of Statistics, University of Wisconsin, Madison, WI, USA. E-mail: zhangzhengjun@ucas.ac.cn.

new endopathic and exopathic competing risk indices for better learning risk patterns, decoupling systemic risk, and making better risk management. The paper establishes the probabilistic properties of stationarity and ergodicity of the AcAF model. Statistical inference is developed through conditional maximum likelihood estimation. The consistency and asymptotic normality of the estimators are derived. Simulation demonstrates the efficiency of the proposed estimators and the AcAF model's flexibility in modeling heterogeneous data. Empirical studies on the stock returns in S&P 500 and the cryptocurrency trading show the superior performance of the proposed model in terms of the identified risk patterns, endopathic and exopathic competing risks, being informative with greater interpretability, enhancing the understanding of the systemic risks of a market and their causes, and making better risk management possible.

Key words and phrases: Business statistics, extreme value analysis, nonlinear time series, risk management, time-varying tail risk

1. Introduction

Systemic risk refers to the risk of collapse of an entire complex system due to the actions taken by the individual component entities or agents that comprise the system. Systemic risk may occur in almost every area, for example, financial crisis, flooding, forest fire, earthquake, market crash, economic crisis, global disease pandemic (like COVID-19), among many others (see Zhang, 2021a,b). Typically, a system contains a number of

risk sources, and once one comes first to collapse, the whole system is affected immediately, i.e., the risk sources are competing. When a disaster event (systemic risk) occurs, it may not be known what causes the event, i.e., its risk source. In such a scenario, it is of significance to decompose systemic risk into competing risks for learning risk patterns and better risk management.

Internal risk refers to the risk from shocks that are generated and amplified within the system. It stands in contrast to external risk, which relates to shocks that arrive from outside the system. Many systems (e.g., social, political, geopolitical, economic, financial, market, regional, global, environmental, transportation, epidemiological, material, chemical, and physical systems) are subject to both types of risk. For instance, the cargo ship MV Ever Given stuck in the Suez Canal on March 26, 2021, faced two major sources of risk. One is its internal operation errors corresponded to internal risk, and the other is strong winds and weather factors contributed to external risk. For more examples of risk decoupling, we refer the readers to Danielsson and Shin (2003).

The occurrence of systemic risk is strongly correlated with extreme events (rare or accumulated). Modeling systemic risk through modeling extreme events is one of the essential topics in risk management. Many

extreme events in history have been associated with systemic risk. Over the past two decades, extreme financial events have repeatedly shown their dramatic and adverse effects on the global economy, which include the Asian financial crisis in 1998, the subprime mortgage crisis of the United States in 2008, the European sovereign debt crisis in 2013, and the “crash” of Chinese stock market in 2015. Failure to recognize these extreme events’ probability makes regulators and practitioners lack effective methods to deal with and prevent the financial crisis. As such, measuring and monitoring extreme financial events’ risk is essential in financial risk management.

Extreme value theory (EVT) has been a powerful tool in risk analysis and is widely applied to model extreme events in finance, insurance, health, climate, and environmental studies (e.g., Embrechts et al. (1999); McNeil and Frey (2000); Poon et al. (2004); Deng et al. (2020)). Extreme events often appeared dynamically and clustered in finance. In the literature, Smith and Goodman (2000), Bali and Weinbaum (2007), Chavez-Demoulin et al. (2014), Kelly and Jiang (2014), Massacci (2017), Zhao et al. (2018), Mao and Zhang (2018), Koo et al. (2020), and Ji and Li (2021) investigate the overall dynamical tail risk structures. In financial applications, Chavez-Demoulin et al. (2016) offers an extreme value theory-based statistical approach for modeling operational risk losses by taking into account

dependence of the parameters on covariates and time; Zhang and Smith (2010) studies multivariate maxima of moving maxima (M4) processes and apply the methodology to model jumps in returns; Daouia et al. (2018) uses the extreme expectiles to measure Value-at-Risk (VaR) and marginal expected shortfall; Harvey (2013) studies the volatility clustering behavior which implies the extreme events' behavior and structure may also change as time goes by.

In the era of Big Data, data may come from multiple sources, and the data from each source has its own generating process, i.e., its probability distribution. The models mentioned above for overall tail risk cannot capture the sources of tail risk accurately. To model extreme values observed from different data sources, there exist some recent studies, e.g., Heffernan et al. (2007), Naveau et al. (2011), Tang et al. (2013), Malinowski et al. (2015), Zhang and Zhu (2016) and Idowu and Zhang (2017). However, these models do not provide insights in risk sources, i.e., they do not differentiate different competing risks. Most recently, the accelerated max-stable distribution has been proposed by Cao and Zhang (2021) to fit the extreme values of data generated from a mixture process (i.e., from different sources), whose mixture patterns vary with the time or sample size. The accelerated max-stable distributions form a new family of extreme value

distributions for modeling maxima of maxima. They provide new probability foundations and statistical tools for modeling competing risks, e.g., endopathic and exopathic competing risks in this paper. These two paired competing risks in our model settings are treated as time-varying tail risks. They show clear paths when clustered disaster events occur, and their interpretations as internal risk and external risk respectively are meaningful both quantitatively and qualitatively in a time series context.

This paper develops an endopathic and exopathic dynamic competing risks model that provides a new tool for better informative and rigorous tail risk analysis. The advantage of our model is to decouple systemic risk into endopathic and exopathic competing risks and measure them. Such decomposition methodology is new to the literature. Our model does not distinguish the data sources a priori, but refines the data's information, characterizes the dynamic tail risk behavior of extreme events through estimated parameter dynamics, and explicitly distinguishes the risk sources, i.e., endopathic risk and exopathic risk. The implementation uses autoregressive conditional accelerated Fréchet (AcAF) distributions to model systemic risks from different sources dynamically. The AcAF model can be applied to financial markets and many other areas where endopathic risk and exopathic risk are intertwined.

This paper makes the following contributions to the growing literature on tail risk measurement in the financial economics and the literature in probability theory and time series, and many applied sciences. First and foremost, we propose a new decoupling risk framework to handle systemic risk. We decouple the systemic risk into endopathic risk and exopathic risk, which is the first based on our knowledge in the field. The AcAF model has two unique features. 1) Although we do not know which data sources the observations come from, the risks from different sources can be reconstructed through the estimated results. 2) The reconstructed parameter dynamics accurately capture the behavior of different risks. Second, the empirical analysis shows our model's superior performance in two financial markets: the U.S. stock market and the Bitcoin trading market. For the U.S. stock market, we find that the dynamics of exopathic risks are more volatile than the dynamics of endopathic risks. Under normal market conditions, endopathic risks (i.e., smaller index values) dominate the stock market price fluctuations, while under turbulent market conditions, exopathic risks dominate. For the Bitcoin trading market, we observe a reverse pattern, i.e., the dynamics of endopathic risks are more volatile than the dynamics of exopathic risks. Exopathic risks dominate the cryptocurrency market price fluctuations under normal market conditions, while

under turbulent market conditions, endopathic risks dominate. We also observe that endopathic risk index values are intermittently but frequently smaller (i.e., dominate) than exopathic risk index values. The apparent opposite phenomena in these two markets are consistent with the actual market structure. Third, our technical proof is non-trivial and can not follow the existing literature's proof directly. They can be applied to other scenarios involving tail processes and parameter dynamics.

The rest of the paper is organized as follows. In Section 2, we introduce the AcAF model and investigate its probabilistic properties. In Section 3, we construct the conditional maximum likelihood estimators (cMLE) for estimation and provide a theory for the estimators' consistency and asymptotic normality. Simulation study on the performance of cMLE is presented in Section 4. In Section 5, we apply our model to three time series of maxima of maxima of negative log-returns in the stock market and Bitcoin market: one on the cross-sectional maximum losses (i.e., negative log-returns) of stocks in S&P 500, one on the intra-day maximum losses of high-frequency trading of GE stock, and the other on the intra-day maximum losses of high-frequency Bitcoin trading. Section 6 gives concluding remarks and discussions. We conclude that the real data results show that our model has a strong ability to portray the endopathic and exopathic risks of the

market and capture the market's dynamic endopathic and exopathic structure. All the technical details and three more simulation studies are given in the supplementary material.

2. Autoregressive conditional accelerated Fréchet model

2.1 Background and motivation

In the era of Big Data, data generated from multiple sources meet in a commonplace. For instance, trading behavior in a market can be different from time to time, e.g., in the morning and the afternoon. Trading behavior in two different markets can be different at the same time. The recorded maximal signal strengths in a brain region can be dynamic, and their source origins can be different from time to time. The maximal precipitations/snowfalls/temperatures in a large area can be dynamic, and their exact locations can be different from time to time. In these examples, the available data are often in a summarized format, e.g., mean, median, low, high, i.e., not all details are given. As a result, the observed extreme values at a given time often come from different latent data sources with different populations. Certainly, the maxima resulted from each individual source has its data generating process, i.e., its limiting extreme value distribution is unique. As such, the classical extreme value theory cannot be directly

2.1 Background and motivation

applied to model the maxima drawn from different populations mixed together. The new EVT for maxima of maxima introduced by Cao and Zhang (2021) provides the probabilistic foundation of accelerated max-stable distribution for studying extreme values of cross-sectional heterogeneous data. We will perform statistical modeling of extreme time series on the basis of this new EVT framework.

The autoregressive conditional Fréchet (AcF) model in Zhao et al. (2018) was the first benchmark model to model cross-sectional maxima through parameter dynamics. It portrays the time series of maxima well. Nevertheless, it does not directly model the heterogeneous data driven by two different risk factors, i.e., endopathic risk dynamics and exopathic risk dynamics. To further advance the new EVT of maxima of maxima and the AcF model, we propose the AcAF model to characterize different sources of tail risks in the financial market, under which a conditional evolution scheme is designed for the parameter $(\mu_t, \sigma_t, \alpha_{1t}, \alpha_{2t})^T$ of accelerated Fréchet distribution, so that time dependency and different risk sources of maxima of maxima can be captured.

2.2 Model specification

Suppose Q_{kt} , $k = 1, \dots, d$ are latent processes, and $Q_t = \max_{1 \leq k \leq d} Q_{kt}$ where each $Q_{kt} = \max_{1 \leq i \leq p_{kt}} X_{k,i,t}$ is again maxima of many time series at time t .

Following Zhao et al. (2018) and Mao and Zhang (2018), we assume

$$Q_{kt} = \mu_{kt} + \sigma_{kt} Y_{kt}^{1/\alpha_{kt}},$$

where μ_{kt} , σ_{kt} and α_{kt} are the location, scale, and shape parameters with Y_{kt} being a unit Fréchet random variable with the distribution function $F(y) = e^{-1/y}$, $y > 0$. Specifically, we consider two latent processes Q_{1t} and Q_{2t} to represent maximum negative log-returns across a group of stocks or of a particular stock's high-frequency trading whose price changes are driven by normal trading behavior and external information (e.g., sentiments), respectively. For example, with normal trading behavior the trading price changes of a particular stock can be higher during the market opening time and the market closing time, and with external information the trading price changes can be quite different from normal trading patterns, i.e., the price changes due to external information can occur at any time. The resulting maximum negative log-returns across that group of stocks or of that particular stock's high-frequency trading can be expressed as $Q_t = \max(Q_{1t}, Q_{2t}) = \max(\max_{1 \leq i \leq p_{1t}} X_{1,i,t}, \max_{1 \leq i \leq p_{2t}} X_{2,i,t})$, where

2.2 Model specification

each $\{X_{k,i,t}\}_{i=1}^{p_{kt}}$, $k = 1, 2$, is a set of time series whose price changes are due to corresponding price change driving factors, respectively.

Note that p_{1t} and p_{2t} are the numbers of transactions, and they can be different and itself can be different from time to time, and the corresponding causes of price changes (negative log-returns) of $X_{1,i,t}$ and $X_{2,i,t}$ cannot be fully determined, i.e., Q_{1t} and Q_{2t} are unobservable latent processes. Here Q_{1t} and Q_{2t} do not correspond to the price changes during the market opening time and the market closing time which were used as a motivating example. They should be understood as they coexist all the time and the dominant one at any given time is observed.

Note that in $Q_t = \max(Q_{1t}, Q_{2t})$, if Q_{1t} and Q_{2t} have different location parameters μ_{1t} and μ_{2t} or different scale parameters σ_{1t} and σ_{2t} , a maximum operator may not be meaningful as one latent component process may not have an effect because the other one always dominates. Also, the theoretical results of maxima of maxima in Cao and Zhang (2021) mainly depend on the tail behaviors of Q_{1t} and Q_{2t} . For model parsimony, we assume $\mu_{1t} = \mu_{2t} = \mu_t$ and follow the literature to assume μ_t as a constant, $\sigma_{1t} = \sigma_{2t} = \sigma_t$, and focus on the dynamics of σ_t , α_{1t} and α_{2t} , which are the pivotal parameters of modeling systemic risk and identifying risk sources. For the rest of the

2.2 Model specification

paper, we consider the following model:

$$Q_t = \max(Q_{1t}, Q_{2t}) = \mu + \sigma_t \max(Y_{1t}^{1/\alpha_{1t}}, Y_{2t}^{1/\alpha_{2t}}), \quad (2.1)$$

$$\log \sigma_t = \beta_0 + \beta_1 \log \sigma_{t-1} - \beta_2 \exp(-\beta_3 Q_{t-1}), \quad (2.2)$$

$$\log \alpha_{1t} = \gamma_0 + \gamma_1 \log \alpha_{1,t-1} + \gamma_2 \exp(-\gamma_3 Q_{t-1}), \quad (2.3)$$

$$\log \alpha_{2t} = \delta_0 + \delta_1 \log \alpha_{2,t-1} + \delta_2 \exp(-\delta_3 Q_{t-1}), \quad (2.4)$$

where $\{Y_{1t}\}$ and $\{Y_{2t}\}$ are sequences of independent and identically distributed (i.i.d.) unit Fréchet random variables. $Y_{1t}^{1/\alpha_{1t}}$ and $Y_{2t}^{1/\alpha_{2t}}$ can be considered as the normal trading driving factor and external information driving factor respectively as mentioned earlier. They compete against each other. The distribution of $\max(Y_{1t}^{1/\alpha_{1t}}, Y_{2t}^{1/\alpha_{2t}})$ in equation (2.1) is called the accelerated Fréchet distribution by Cao and Zhang (2021). In addition, $\beta_0, \gamma_0, \delta_0, \mu \in \mathbb{R}$, $0 \leq \beta_1 \neq \gamma_1 \neq \delta_1 < 1$ and $\beta_2, \beta_3, \gamma_2, \gamma_3, \delta_2, \delta_3 > 0$ are assumed for the model to be stationary and technical requirements.

For model estimation identifiability, we assume $\text{var}(\gamma_2 \exp(-\gamma_3 Q_{t-1})) > \text{var}(\delta_2 \exp(-\delta_3 Q_{t-1}))$.

Remark 1. Note that although $\beta_2, \gamma_2, \delta_2$ are all assumed greater than zero, they can be set as zero. As long as any of them are set to be zero, all theories and estimation methods developed can be easily adjusted because the corresponding dynamic equations will become constants. For example,

2.2 Model specification

assuming $\gamma_2 = 0$, then the dynamic equation (2.3) will result in a stationary solution of $\alpha_{1t} = \exp(\gamma_0/(1 - \gamma_1))$. This paper will not separately develop additional theoretical results for any of β_2 , γ_2 , and δ_2 being zero as we will have a simplified model with the corresponding α_{1t} as a constant in Section 5.2.

Remark 2. Note that Q_t needs not to express as $\max(Q_{1t}, Q_{2t})$ in equation (2.1), i.e., we can directly express $Q_t = \mu + \sigma_t \max(Y_{1t}^{1/\alpha_{1t}}, Y_{2t}^{1/\alpha_{2t}})$. In addition, we only observe one univariate time series Q_t , i.e., a standardized function $(Q_t - \mu)/\sigma_t$ follows an accelerated Fréchet distribution. Therefore, it should not be understood as our model is for a bivariate time series with two different σ_{1t} and σ_{2t} .

Before introducing our proposed endopathic and exopathic risk indices in a time series context, let's consider an illustrative example of widely studied endogenous and exogenous variables in the literature of economic modeling. Suppose Y is a dependent variable, X_1 is an independent variable, and $X_2 = g(X_1)$ with $g(\cdot)$ being a Borel measurable function and $\text{var}(X_1) \neq \text{var}(X_2)$. Suppose Y can be expressed as

$$Y = X_1 + \epsilon = g(X_1) + (X_1 - g(X_1) + \epsilon) =: X_2 + \epsilon^*,$$

with X_1 and ϵ being uncorrelated. Obviously, X_2 and ϵ^* are correlated.

2.2 Model specification

Then X_1 is an exogenous variable, X_2 is an endogenous variable, and clearly $\text{var}(\epsilon^*) > \text{var}(\epsilon)$ regardless whether $\text{var}(X_1) > \text{var}(X_2)$ or $\text{var}(X_1) < \text{var}(X_2)$.

Using the above illustrative example, it is easy to see that the lag-1 variable in an AR(1) model is an exogenous variable when the model is correctly specified. However, the primary interest of nonlinear time series models (2.1) - (2.4) is to model tail risk dynamics, hence we cannot directly extend the use of endogenous and exogenous variables in our new modeling framework. Therefore, motivated by the above illustrative example, we define two new tail risk indices next.

Definition 1. Under the model identifiability condition, i.e.,

$$\text{var}(\gamma_2 \exp(-\gamma_3 Q_{t-1})) > \text{var}(\delta_2 \exp(-\delta_3 Q_{t-1})), \quad (2.5)$$

$\alpha_{1,t-1}$ is referred as the tail endopathic risk index (for simplicity, call it endopathic risk) of Q_{t-1} , and relative to endopathic risk, $\alpha_{2,t-1}$ is referred as the tail exopathic risk index (for simplicity, call it exopathic risk) of Q_{t-1} .

Note that endopathic and exopathic risks coexist dynamically; however, endogenous and exogenous variables may not. In addition, endopathic risks are caused by internal errors, while exopathic risks are caused by external information (e.g., market sentiments). Both internal (error) information and

2.2 Model specification

external (error) information may not be measurable, and they are derived by the model expressed as $\gamma_2 \exp(-\gamma_3 Q_{t-1})$ and $\delta_2 \exp(-\delta_3 Q_{t-1})$, respectively. Due to the coexistence of the two risks, they can be dependent and interact with each other, which is reflected in their definitions and models. We further note that the identifiability condition is a probabilistic condition, i.e., a population condition, and not a statistical condition, which follows the same idea as what endogenous and exogenous were defined. In the real data section, we use three examples to empirically and perfectly justify the validity of the definitions.

Remark 3. The economic modeling literature commonly decomposes risks into two categories: endogenous (internal) and exogenous (external), see Danielsson and Shin (2003). However, to the best of our knowledge, currently, there do not exist statistical measures for distinguishing between these two types of risks. Also, there do not exist explicit definitions for the two risk measures in the field of risk management that correspond to “endogenous” and “exogenous” in economics. With the introduction of the risk competing idea and the model structure, the AcAF model makes defining and decoupling systemic risk into endogenous and exogenous risks possible. In the AcAF model, we adopt the concepts of “endopathic risk” and “exopathic risk” which are defined for time series with clustered ex-

2.2 Model specification

treme events, and their interpretations are motivated but different from endogenous variable and exogenous variable. Endopathic risk corresponds to the endogenous (internal) risk while exopathic risk corresponds to the exogenous (external) risk. Given risks are often referred to the tail regions.

In Definition 1, we define tail endopathic risk index and tail exopathic risk index by drawing analogies with endogenous and exogenous variables in economics.

Remark 4. Note that the identifiability condition (2.5) is not a technical condition and is not necessary. Without this condition, we can still estimate the parameters of the AcAF model accurately, and α_{1t} and α_{2t} are exchangeable. In fact, exchanging α_{1t} and α_{2t} does not affect the probabilistic properties of the data generating process due to Y_{1t} and Y_{2t} are independent and identically distributed unit Fréchet random variables. As such, we obtain two equivalent models after fitting the data, which means α_{1t} can be treated as α_{2t} , and vice versa. Mathematically speaking, making the condition of (2.5) is just for mathematical convenience, i.e., it's not a technical condition. Economically speaking, this condition leads to our financially interpretable definition of the tail endopathic risk index (endopathic risk) and the tail exopathic risk index (exopathic risk), see Definition 1.

2.2 Model specification

Remark 5. Note that the tail properties of the endopathic and exopathic risks are influenced by various factors. The performance of the time series model (2.2)-(2.4) is highly correlated with both the first-order autoregressive coefficients and the intercept terms, which must be considered in conjunction with the error terms. Therefore, the model can exhibit varying characteristics in different markets. In the real market, the tail risk always exists. The endopathic risk and the exopathic risk intersect and the dominant risk changes over time. The tail properties of the two risks can be further explained by the empirical results in Section 5. The observations reflect the qualitative analysis of the two types of markets, and demonstrate the AcAF model's strong ability to accurately represent the tail properties of two risks inherent in the market.

Remark 6. In the model (2.1)-(2.4), we set $\alpha_{it}, i = 1, 2$. A natural question will be why not make $i = 1, 2, \dots, k$ with $k > 2$. Of course, making $k > 2$ can be done theoretically and the probabilistic properties of the model can still hold. However, $k > 2$ will increase statistical inference complexity and estimation inefficiency, e.g., in optimization problems. In the economic modeling literature, risks are often decoupled into two main risks, i.e., internal and external risks, for easy interpretability, e.g., Danielsson and Shin (2003), Farboodi et al. (2021), Lopez and Saidenberg (2000). Certainly,

2.2 Model specification

internal (external) risk can further be decoupled into more specific risks, which can be challenging. Following the economic modeling literature, we set $k = 2$ in this paper.

We note that the autoregressive structures used in σ_t , α_{1t} and α_{2t} can be traced back to GARCH model in Bollerslev (1986), autoregressive conditional density model in Hansen (1994), and autoregressive conditional durational model in Engle and Russell (1998). The clustering of extreme events in time is a significant feature of the extreme value series $\{Q_t\}$ in many applications, especially in financial time series. Empirical evidences have shown that extreme observations tend to happen around the same period in many applications. Translating this phenomenon in our model, we can say that an extreme event observed at time $t - 1$ causes the distribution of Q_t to have larger scale (larger σ_t) and heavier tail (smaller tail index), resulting in a larger tail risk of Q_t . Here, a smaller tail index implies a larger tail risk. In Section 2.4, we present a class of factor models and show the limiting distribution of maxima of maxima of the response variables to be the accelerated Fréchet types.

The σ_t in (2.1) can be thought as volatility, i.e., analog to what is called in GARCH models. Writing (2.1) in the following equivalent equation:

$$\log(Q_t - \mu) = \log(\sigma_t) + \max\{1/\alpha_{1t} \log(Y_{1t}), 1/\alpha_{2t} \log(Y_{2t})\}.$$

2.2 Model specification

Then $\log(\sigma_t)$ becomes location parameters, while $1/\alpha_{1t}$ and $1/\alpha_{2t}$ become a pair of scale parameters or super-volatilities to distinct them from the regular volatility definition. We can immediately see that the smaller the α_{1t} , the larger the super-volatility (the risk), and the same is true for α_{2t} .

Remark 7. To describe the dynamics of the risk factors from different sources, we extend the one-component AcF model (Zhao et al. (2018)) into the two-component AcAF model. This advance is like advancing the ARCH model to the GARCH model in the literature. We further think about the risk reality in the market being driven by two main types of risks: internal and external. As such, it may be safe to say that a model with two component risks (internal and external) should be pursued, while a one-component risk model is still useful given it may integrate all sources of risks into one risk. In S5.2 of the supplementary file, we conduct simulations to compare the performance between the AcF and the AcAF models.

Remark 8. From the theoretical perspective, due to the complexity of nonlinear time series, even when $\alpha_{1t} = \alpha_{2t} = \alpha_t$, the AcAF model cannot degenerate into the AcF model. Because $\max(Y_{1t}^{1/\alpha_t}, Y_{2t}^{1/\alpha_t}) \stackrel{d}{=} (2Y_t)^{1/\alpha_t}$, where Y_{1t}, Y_{2t} , and Y_t are all independent unit Fréchet random variables, and $P(\max(Y_{1t}^{1/\alpha_t}, Y_{2t}^{1/\alpha_t}) \leq x) = \exp[-\{(x - 0)/(2^{1/\alpha_t})\}^{-\alpha_t}]$. Then $(Q_t - \mu_t)/\sigma_t = \max(Y_{1t}^{1/\alpha_t}, Y_{2t}^{1/\alpha_t}) \sim \text{Fréchet}(0, 2^{1/\alpha_t}, \alpha_t)$, which indicates that the

2.3 Stationarity and ergodicity

standardized maxima of maxima follows Fréchet distribution with location parameter 0, scale parameter $2^{1/\alpha_t}$, and shape parameter α_t . Then we obtain that the scale parameter of Q_t 's distribution is $2^{1/\alpha_t}\sigma_t$, which depends on the shape parameter α_t . Hence the dynamic structure of the scale parameter in the AcAF model will be different from the dynamic structure of the scale parameter in the AcF model. So the AcF model cannot be regarded as a special case of the AcAF model even with $\alpha_{1t} = \alpha_{2t}$.

2.3 Stationarity and ergodicity

The evolution schemes (2.2)-(2.4) can be written as

$$\log \sigma_t = \beta_0 + \beta_1 \log \sigma_{t-1} - \beta_2 \exp[-\beta_3 \{\mu + \sigma_{t-1} \max(Y_{1,t-1}^{1/\alpha_{1,t-1}}, Y_{2,t-1}^{1/\alpha_{2,t-1}})\}], \quad (2.6)$$

$$\log \alpha_{1t} = \gamma_0 + \gamma_1 \log \alpha_{1,t-1} + \gamma_2 \exp[-\gamma_3 \{\mu + \sigma_{t-1} \max(Y_{1,t-1}^{1/\alpha_{1,t-1}}, Y_{2,t-1}^{1/\alpha_{2,t-1}})\}], \quad (2.7)$$

$$\log \alpha_{2t} = \delta_0 + \delta_1 \log \alpha_{2,t-1} + \delta_2 \exp[-\delta_3 \{\mu + \sigma_{t-1} \max(Y_{1,t-1}^{1/\alpha_{1,t-1}}, Y_{2,t-1}^{1/\alpha_{2,t-1}})\}]. \quad (2.8)$$

Hence $\{\sigma_t, \alpha_{1t}, \alpha_{2t}\}$ forms a homogeneous Markov chain in \mathbb{R}^3 . The following theorem provides a sufficient condition under which the process $\{\sigma_t, \alpha_{1t}, \alpha_{2t}\}$ is stationary and ergodic.

2.4 AcAF model under a factor model setting

Theorem 1. *For the AcAF model with $\beta_0, \gamma_0, \delta_0, \mu \in \mathbb{R}$, $\beta_2, \beta_3, \gamma_2, \gamma_3, \delta_2, \delta_3 > 0$, and $0 \leq \beta_1 \neq \gamma_1 \neq \delta_1 < 1$, the latent process $\{\sigma_t, \alpha_{1t}, \alpha_{2t}\}$ is stationary and geometrically ergodic.*

The proof of Theorem 1 can be found in the supplement. In the process of proving ergodicity, the sequence Q_t is driven by two random variables Y_{1t} and Y_{2t} alternately, which brings new challenges to the proof due to the additional max nonlinear operator. The technical difficulty is that there is no one-to-one relationship between Q_t and Y_t like in Zhao et al. (2018). Our proof extends the theoretical result to a dynamic model for nonlinear time series driven by two variables. We note that this is the first formal treatment for stationarity and ergodicity of nonlinear time series driven by two variables under extreme value framework. Since $\{Q_t\}$ is a coupled process of $\{\sigma_t, \alpha_{1t}, \alpha_{2t}\}$ through (2.1), $\{Q_t\}$ is also stationary and ergodic.

2.4 AcAF model under a factor model setting

In this section, we show that the limiting distribution of maxima Q_t under a factor model framework coincides with the accelerated Fréchet distribution of an AcAF model. We assume both $\{X_{1,i,t}\}_{i=1}^{p_{1t}}$ and $\{X_{2,j,t}\}_{j=1}^{p_{2t}}$ follow

2.4 AcAF model under a factor model setting

general factor models,

$$X_{1,i,t} = f_i(Z_{1t}, Z_{2t}, \dots, Z_{dt}) + \sigma_{it}\epsilon_{1,i,t},$$

$$X_{2,j,t} = \tilde{f}_j(Z_{1t}, Z_{2t}, \dots, Z_{dt}) + \tilde{\sigma}_{jt}\epsilon_{2,j,t},$$

where $\{X_{1,i,t}\}_{i=1}^{p_{1t}}$ and $\{X_{2,j,t}\}_{j=1}^{p_{2t}}$ are two latent time series at time t , $\{Z_{1t}, Z_{2t}, \dots, Z_{dt}\}$ consist of observed and unobserved factors, $\{\epsilon_{1,i,t}\}_{i=1}^{p_{1t}}$ and $\{\epsilon_{2,j,t}\}_{j=1}^{p_{2t}}$ are two i.i.d. random noises that are independent to each other and independent with the factors $\{Z_{it}\}_{i=1}^d$, and $\{\sigma_{it}\}_{i=1}^{p_{1t}}, \{\tilde{\sigma}_{jt}\}_{j=1}^{p_{2t}} \in \mathcal{F}_{t-1}$ are the conditional volatilities of $\{X_{1,i,t}\}_{i=1}^{p_{1t}}$ and $\{X_{2,j,t}\}_{j=1}^{p_{2t}}$, respectively. The functions $f_i, \tilde{f}_j : \mathbb{R}^d \rightarrow \mathbb{R}$ are Borel functions. Without misunderstanding, we use p_1 and p_2 to denote p_{1t} and p_{2t} , respectively.

One fundamental characteristic of many financial time series is that they are often heavy-tailed. To incorporate this observation, we make the common assumption that the random noises $\{\epsilon_{1,i,t}\}_{i=1}^{p_1}$ and $\{\epsilon_{2,j,t}\}_{j=1}^{p_2}$ are i.i.d. random variables in the Domain of Attraction of Fréchet distribution (Leadbetter et al., 1983). Here and after, for two positive functions $m_1(x)$ and $m_2(x)$, $m_1(x) \sim m_2(x)$ means $\frac{m_1(x)}{m_2(x)} \rightarrow 1$, as $x \rightarrow \infty$. Specifically, we adopt the following definition.

Definition 2 (Domain of Attraction of Fréchet distribution). A random variable ϵ is in the Domain of Attraction of Fréchet distribution with tail index α if and only if $x_F = \infty$ and $1 - F_\epsilon \sim l(x)x^{-\alpha}$, $\alpha > 0$, where F_ϵ is

2.4 AcAF model under a factor model setting

the cumulative distribution function (c.d.f.) of ϵ , $l(x)$ is a slowly-varying function and $x_F = \sup\{x : F_\epsilon(x) < 1\}$.

Domain of Attraction of Fréchet distribution includes a broad class of distributions such as Cauchy, Burr, Pareto and t distributions. To facilitate algebraic derivation, we further assume that for slowly varying functions corresponding to $\{\epsilon_{1,i,t}\}_{i=1}^{p_1}$ and $\{\epsilon_{2,j,t}\}_{j=1}^{p_2}$ respectively, $l_{1t}(x) \rightarrow K_{1t}$ and $l_{2t}(x) \rightarrow K_{2t}$ as $x \rightarrow \infty$, where $K_{1t}, K_{2t} \in \mathcal{F}_{t-1}$ are two positive constants. This is a rather weak assumption with all the aforementioned distributions satisfying this condition. Since K_{1t} and K_{2t} can be incorporated into each σ_{it} , without loss of generality, we set K_{1t} and K_{2t} are both equal to 1 in the following. Under a dynamic model, we assume that the conditional tail indices α_{1t} and α_{2t} of $\epsilon_{1,i,t}$ and $\epsilon_{2,j,t}$ respectively evolve through time according to certain dynamics (e.g., (2.3) and (2.4)) and $\alpha_{1t}, \alpha_{2t} \in \mathcal{F}_{t-1}$.

We also assume that

$$\sup_{1 \leq p_1 < \infty} \sup_{1 \leq i \leq p_1} |f_i(Z_{1t}, Z_{2t}, \dots, Z_{dt})| < \infty, \text{ a.s.}$$

and that

$$\sup_{1 \leq p_2 < \infty} \sup_{1 \leq j \leq p_2} |\tilde{f}_j(Z_{1t}, Z_{2t}, \dots, Z_{dt})| < \infty, \text{ a.s.}$$

Notice here the supremum is taken over p_1 or p_2 with the number of latent factors d fixed. This is a mild assumption and it includes all the com-

2.4 AcAF model under a factor model setting

monly encountered factor models. For example, if the factor model takes a linear form, $f_i(Z_{1t}, \dots, Z_{dt}) = \sum_{s=1}^d \beta_s^{(i)} Z_{st}$, a sufficient condition for the assumption to hold would be $\sup_{1 \leq p_1 < \infty} \sup_{1 \leq i \leq p_1} \|\boldsymbol{\beta}^{(i)}\| < \infty$, where $\boldsymbol{\beta}^{(i)} = (\beta_1^{(i)}, \dots, \beta_d^{(i)})^T$. We further assume that there exist positive constants C_1 and C_2 such that $C_1 \leq \sigma_{it}, \tilde{\sigma}_{jt} \leq C_2$ for any $p_1, p_2, 1 \leq i \leq p_1$ and $1 \leq j \leq p_2$.

Based on Proposition 1 in Zhao et al. (2018), given \mathcal{F}_{t-1} , we have, as $p_1 \rightarrow \infty, p_2 \rightarrow \infty$,

$$\frac{\max_{1 \leq i \leq p_1} \{X_{1,i,t}\} - b_{1,p_1,t}}{a_{1,p_1,t}} \xrightarrow{d} \Psi_{\alpha_{1t}} \quad \text{and} \quad \frac{\max_{1 \leq j \leq p_2} \{X_{2,j,t}\} - b_{2,p_2,t}}{a_{2,p_2,t}} \xrightarrow{d} \Psi_{\alpha_{2t}},$$

where $a_{1,p_1,t} = (\sum_{i=1}^{p_1} \sigma_{it}^{\alpha_{1t}})^{1/\alpha_{1t}}$, $a_{2,p_2,t} = (\sum_{j=1}^{p_2} \tilde{\sigma}_{jt}^{\alpha_{2t}})^{1/\alpha_{2t}}$, $b_{1,p_1,t} = b_{2,p_2,t} = 0$, $\Psi_{\alpha_{1t}}(x) = \exp(-x^{-\alpha_{1t}})$ and $\Psi_{\alpha_{2t}}(x) = \exp(-x^{-\alpha_{2t}})$ denote the distributions of Fréchet type random variables with tail indices $\alpha_{1t} > 0$ and $\alpha_{2t} > 0$, respectively.

Recall that $Q_t = \max(Q_{1t}, Q_{2t}) = \max(\max_{1 \leq i \leq p_1} X_{1,i,t}, \max_{1 \leq j \leq p_2} X_{2,j,t})$. The limiting distribution form of Q_t needs some discussions about the size of two tail indices and the order of p_1 and p_2 .

Proposition 1. *Given \mathcal{F}_{t-1} , under the assumptions in this section, the limiting distribution of Q_t as $p_1, p_2 \rightarrow \infty$ can be determined in the following cases:*

2.4 AcAF model under a factor model setting

Case 1. $\alpha_{1t} < \alpha_{2t}$.

1. If $p_1/p_2 \rightarrow C > 0$ or ∞ , then $a_{1,p_1,t}/a_{2,p_2,t} \rightarrow \infty$ and $P\left(\frac{Q_t - b_{1,p_1,t}}{a_{1,p_1,t}} \leq x\right) \rightarrow \Psi_{\alpha_{1t}}(x)$.
2. If $p_1/p_2 \rightarrow 0$ and $a_{1,p_1,t}/a_{2,p_2,t} \rightarrow a_t > 0$, then $P\left(\frac{Q_t - b_{1,p_1,t}}{a_{1,p_1,t}} \leq x\right) \rightarrow \Psi_{\alpha_{1t}}(x)\Psi_{\alpha_{2t}}(a_t x)$.

Case 2. $\alpha_{1t} = \alpha_{2t} = \alpha_t$.

1. If $p_1/p_2 \rightarrow C > 0$ and $a_{1,p_1,t}/a_{2,p_2,t} \rightarrow a_t > 0$, then $P\left(\frac{Q_t - b_{1,p_1,t}}{a_{1,p_1,t}} \leq x\right) \rightarrow \Psi_{\alpha_t}(x)\Psi_{\alpha_t}(a_t x)$.
2. If $p_1/p_2 \rightarrow 0$, then $a_{1,p_1,t}/a_{2,p_2,t} \rightarrow 0$ and $P\left(\frac{Q_t - b_{2,p_2,t}}{a_{2,p_2,t}} \leq x\right) \rightarrow \Psi_{\alpha_t}(x)$.
3. If $p_1/p_2 \rightarrow \infty$, then $a_{1,p_1,t}/a_{2,p_2,t} \rightarrow \infty$ and $P\left(\frac{Q_t - b_{1,p_1,t}}{a_{1,p_1,t}} \leq x\right) \rightarrow \Psi_{\alpha_t}(x)$.

Case 3. $\alpha_{1t} > \alpha_{2t}$.

1. If $p_1/p_2 \rightarrow C \geq 0$, then $a_{1,p_1,t}/a_{2,p_2,t} \rightarrow 0$ and $P\left(\frac{Q_t - b_{2,p_2,t}}{a_{2,p_2,t}} \leq x\right) \rightarrow \Psi_{\alpha_{2t}}(x)$.
2. If $p_1/p_2 \rightarrow \infty$ and $a_{2,p_2,t}/a_{1,p_1,t} \rightarrow a_t > 0$, then $P\left(\frac{Q_t - b_{2,p_2,t}}{a_{2,p_2,t}} \leq x\right) \rightarrow \Psi_{\alpha_{1t}}(a_t x)\Psi_{\alpha_{2t}}(x)$.

2.4 AcAF model under a factor model setting

The proof of Proposition 1 can be found in the supplement.

Under a particular setup, we assume $p_1 = p_2 = p$ and denote $f_i(Z_{1t}, Z_{2t}, \dots, Z_{dt}) = \tilde{f}_i(Z_{1t}, Z_{2t}, \dots, Z_{dt})$ as the underlying return values of the i th stock, $X_{1,i,t}$ (or $X_{2,i,t}$) as the unobserved value of the i th stock when the endopathic shock is stronger (weaker) than the exopathic shock. Under this setting, we can rewrite the observed time series Q_t as

$$\begin{aligned} Q_t &= \max(X_{1t}, X_{2t}) = \max\left(\max_{1 \leq i \leq p} X_{1,i,t}, \max_{1 \leq i \leq p} X_{2,i,t}\right) \\ &= \max\left[\max_{1 \leq i \leq p} \left\{f_i(Z_{1t}, Z_{2t}, \dots, Z_{dt}) + \sigma_{it}\epsilon_{1,i,t}\right\}, \max_{1 \leq i \leq p} \left\{f_i(Z_{1t}, Z_{2t}, \dots, Z_{dt}) + \sigma_{it}\epsilon_{2,i,t}\right\}\right] \\ &= \max_{1 \leq i \leq p} \left[\max\left\{f_i(Z_{1t}, Z_{2t}, \dots, Z_{dt}) + \sigma_{it}\epsilon_{1,i,t}, f_i(Z_{1t}, Z_{2t}, \dots, Z_{dt}) + \sigma_{it}\epsilon_{2,i,t}\right\}\right] \\ &= \max_{1 \leq i \leq p} \left\{f_i(Z_{1t}, Z_{2t}, \dots, Z_{dt}) + \sigma_{it} \max(\epsilon_{1,i,t}, \epsilon_{2,i,t})\right\}. \end{aligned}$$

Corollary 1 gives the general asymptotic conditional distribution of maxima Q_t when p goes to infinity.

Corollary 1. Denote $a_{j,p,t} = \left(\sum_{i=1}^p \sigma_{it}^{\alpha_{jt}}\right)^{1/\alpha_{jt}}$, and $b_{j,p,t} = 0$ for $j = 1, 2$.

Given \mathcal{F}_{t-1} , the limiting distribution of Q_t as $p \rightarrow \infty$ can be determined in the following cases:

1. If $\alpha_{1t} < \alpha_{2t}$, then $a_{1,p,t}/a_{2,p,t} \rightarrow \infty$, and $P\left(\frac{Q_t - b_{1,p,t}}{a_{1,p,t}} \leq x\right) \rightarrow \Psi_{\alpha_{1t}}(x)$.
2. If $\alpha_{1t} = \alpha_{2t} = \alpha_t$, then $a_{1,p,t} = a_{2,p,t}$, and $P\left(\frac{Q_t - b_{1,p,t}}{a_{1,p,t}} \leq x\right) \rightarrow \Psi_{\alpha_t}(x)\Psi_{\alpha_t}(x)$.

3. If $\alpha_{1t} > \alpha_{2t}$, then $a_{1,p,t}/a_{2,p,t} \rightarrow 0$, and $P\left(\frac{Q_t - b_{2,p,t}}{a_{2,p,t}} \leq x\right) \rightarrow \Psi_{\alpha_{2t}}(x)$.

Both Proposition 1 and Corollary 1 show that under the framework of the general factor model and some mild conditions, the conditional distribution of maxima Q_t can be well approximated by an accelerate Fréchet distribution. In terms of stochastic representation, the observed maxima value Q_t can be rewritten as $Q_t \approx \sigma_t \max(Y_{1t}^{1/\alpha_{1t}}, Y_{2t}^{1/\alpha_{2t}})$, where Y_{1t} and Y_{2t} are two independent unit Fréchet random variables and σ_t depends on the size of α_{1t} and α_{2t} . More specifically, if $\alpha_{1t} < \alpha_{2t}$, then $\sigma_t = \lim_{p \rightarrow \infty} a_{1,p,t}$; if $\alpha_{1t} > \alpha_{2t}$, then $\sigma_t = \lim_{p \rightarrow \infty} a_{2,p,t}$; if $\alpha_{1t} = \alpha_{2t}$, then $\sigma_t = \lim_{p \rightarrow \infty} a_{1,p,t} = \lim_{p \rightarrow \infty} a_{2,p,t}$. To be more flexible and accurate in finite samples, a location parameter μ_t can be included. That is,

$$Q_t \approx \mu_t + \sigma_t \max(Y_{1t}^{1/\alpha_{1t}}, Y_{2t}^{1/\alpha_{2t}}),$$

where $\{\mu_t, \sigma_t, \alpha_{1t}, \alpha_{2t}\}$ are time-varying parameters. Setting $\mu_t = \mu$ for parsimonious modeling, we obtain the dynamic structure of $\{Q_t\}$ specified in (2.1).

3. Parameter estimation

We denote all the parameters in the model by

$$\boldsymbol{\theta} = (\beta_0, \beta_1, \beta_2, \beta_3, \gamma_0, \gamma_1, \gamma_2, \gamma_3, \delta_0, \delta_1, \delta_2, \delta_3, \mu)^T,$$

and denote the parameter space by

$$\Theta_s = \{\boldsymbol{\theta} | \beta_0, \gamma_0, \delta_0, \mu \in \mathbb{R}, 0 \leq \beta_1, \gamma_1, \delta_1 \leq 1, \beta_2, \beta_3, \gamma_2, \gamma_3, \delta_2, \delta_3 > 0\}.$$

In the following, we assume that all allowable parameters are in Θ_s and the

true parameter is $\boldsymbol{\theta}_0 = (\beta_0^0, \beta_1^0, \beta_2^0, \beta_3^0, \gamma_0^0, \gamma_1^0, \gamma_2^0, \gamma_3^0, \delta_0^0, \delta_1^0, \delta_2^0, \delta_3^0, \mu_0)^T$.

The conditional probability density function (p.d.f.) of Q_t given $(\mu, \sigma_t, \alpha_{1t}, \alpha_{2t})^T$ is

$$\begin{aligned} f_t(\boldsymbol{\theta}) &= \{\alpha_{1t}\sigma_t^{\alpha_{1t}}(Q_t - \mu)^{-\alpha_{1t}-1} + \alpha_{2t}\sigma_t^{\alpha_{2t}}(Q_t - \mu)^{-\alpha_{2t}-1}\} \\ &\quad \times \exp\{-\sigma_t^{\alpha_{1t}}(Q_t - \mu)^{-\alpha_{1t}} - \sigma_t^{\alpha_{2t}}(Q_t - \mu)^{-\alpha_{2t}}\}. \end{aligned} \quad (3.1)$$

By conditional independence, the log-likelihood function with observations $\{Q_t\}_{t=1}^n$ is

$$\begin{aligned} L_n(\boldsymbol{\theta}) &= \frac{1}{n} \sum_{t=1}^n l_t(\boldsymbol{\theta}) = \frac{1}{n} \sum_{t=1}^n \left[\log \{\alpha_{1t}\sigma_t^{\alpha_{1t}}(Q_t - \mu)^{-\alpha_{1t}-1} + \alpha_{2t}\sigma_t^{\alpha_{2t}}(Q_t - \mu)^{-\alpha_{2t}-1}\} \right. \\ &\quad \left. - \sigma_t^{\alpha_{1t}}(Q_t - \mu)^{-\alpha_{1t}} - \sigma_t^{\alpha_{2t}}(Q_t - \mu)^{-\alpha_{2t}} \right], \end{aligned} \quad (3.2)$$

where $\{\sigma_t, \alpha_{1t}, \alpha_{2t}\}_{t=1}^n$ can be obtained recursively through (2.2)-(2.4), with an initial value $(\sigma_1, \alpha_{11}, \alpha_{21})^T$.

Denote the log-likelihood function based on an arbitrary initial value $(\tilde{\sigma}_1, \tilde{\alpha}_{11}, \tilde{\alpha}_{21})^T$ as $\tilde{L}_n(\boldsymbol{\theta})$. Theorems 2 and 3 show that there always exists a sequence $\hat{\boldsymbol{\theta}}_n$, which is a local maximizer of $\tilde{L}_n(\boldsymbol{\theta})$, such that $\hat{\boldsymbol{\theta}}_n$ is consistent and asymptotically normal, regardless of the initial value $(\tilde{\sigma}_1, \tilde{\alpha}_{11}, \tilde{\alpha}_{21})^T$.

Theorem 2 (Consistency). *Assume Θ is a compact set of Θ_s . Suppose the observations $\{Q_t\}_{t=1}^n$ are generated by a stationary and ergodic model with true parameter θ_0 and θ_0 is in the interior of Θ , then there exists a sequence $\hat{\theta}_n$ of local maximizer of $\tilde{L}_n(\theta)$ such that $\hat{\theta}_n \rightarrow_p \theta_0$ and $\|\hat{\theta}_n - \theta_0\| \leq \tau_n$, where $\tau_n = O_p(n^{-r})$, $0 < r < 1/2$. Hence $\hat{\theta}_n$ is consistent.*

Theorem 2 shows that there exists a sequence $\hat{\theta}_n$ which contains not only consistent cMLE to θ_0 but also local maximizer of $\tilde{L}_n(\theta)$. Next, we derive the asymptotic distributions of our estimators $\hat{\theta}_n$ in the following Theorem 3.

Theorem 3 (Asymptotic normality). *Under the conditions in Theorem 2, we have $\sqrt{n}(\hat{\theta}_n - \theta_0) \xrightarrow{d} N(\mathbf{0}, \mathbf{M}_0^{-1})$, where $\hat{\theta}_n$ is given in Theorem 2 and \mathbf{M}_0 is the Fisher Information matrix evaluated at θ_0 . Further, the sample variance-covariance matrix of plug-in estimated score functions $\{\frac{\partial}{\partial \theta} l_t(\hat{\theta}_n)\}_{t=1}^n$ is a consistent estimator of \mathbf{M}_0 .*

Although the consistency of $\hat{\theta}_n$ and their asymptotic distributions are shown in Theorem 2 and Theorem 3 respectively, the uniqueness of cMLE remains open due to the complexity brought by μ . Proposition 2 provides a segmentary answer to the uniqueness of cMLE.

Proposition 2 (Asymptotic uniqueness). *Denote $V_n = \{\theta \in \Theta | \mu \leq cQ_{n,1} +$*

$(1 - c)\mu_0\}$ where $Q_{n,1} = \min_{1 \leq t \leq n} Q_t$, under the conditions in Theorem 2, for any fixed $0 < c < 1$. There exists a sequence of $\hat{\boldsymbol{\theta}}_n = \arg \max_{\boldsymbol{\theta} \in V_n} \tilde{L}_n(\boldsymbol{\theta})$ such that, $\hat{\boldsymbol{\theta}}_n \rightarrow_p \boldsymbol{\theta}_0$, $\|\hat{\boldsymbol{\theta}}_n - \boldsymbol{\theta}_0\| \leq \tau_n$ where $\tau_n = O_p(n^{-r})$ with $0 < r < 1/2$, and

$$P(\hat{\boldsymbol{\theta}}_n \text{ is the unique global maximizer of } \tilde{L}_n(\boldsymbol{\theta}) \text{ over } V_n) \rightarrow 1.$$

The proofs of Theorems 2 and 3 and Proposition 2 can be found in the supplement. Since the sequence Q_t is driven by two different Fréchet types of latent processes alternately, the benchmark structure and proofs in Zhao et al. (2018) need to be substantially modified, which is nontrivial. In addition, we add some probability equations to analyze the consistency and asymptotic normality of nonlinear time series driven by two variables.

4. Simulation study

In this section, we study the finite sample performance of the cMLE under the AcAF model. More simulation studies on “Performance of the cMLE under X_{it} in the max domain of attraction”, “Comparison with the autoregressive conditional Fréchet model”, and “Convergence of maxima of maxima in factor model” are given in S5.1, S5.2, and S5.3, respectively, of the supplementary file.

We generate data from the AcAF model with the following parameters

$(\beta_0, \beta_1, \beta_2, \beta_3, \gamma_0, \gamma_1, \gamma_2, \gamma_3, \delta_0, \delta_1, \delta_2, \delta_3, \mu)^T = (-0.244, 0.787, 0.066, 8.111, 0.230, 0.755, 0.417, 7.114, -0.035, 0.907, 0.425, 4.861, -0.227)^T$. This set of parameters is obtained from the real data analysis of the S&P 500 daily negative log-returns using the AcAF model. Under this setting, the typical range of α_{1t} is $[3.26, 10.17]$, the typical range of α_{2t} is $[2.68, 26.94]$, and the typical range of σ_t is $[0.25, 0.31]$.

We investigate the performance of cMLE with sample sizes $N = 1000, 2000, 5000, 10000$. For each sample size, we conduct 100 experiments. The results for parameter estimation are in Table 1, including the average of the estimates and the standard deviation from the 100 experiments. From Table 1, we can see that both the bias and variance of the cMLE decrease as the sample size N increases, demonstrating the consistency of the cMLE under correct model specification. We find that the performance of cMLE is already satisfactory when $N = 5000$.

5. Real data applications

In this section, we present three real data applications of the AcAF model, one on the cross-sectional maxima of negative log-returns of stocks in S&P 500, one on the intra-day maxima of negative log-returns from high-frequency stock trading, and the other on the intra-day maxima of negative log-returns

Decoupling Systemic Risk

Table 1: Numerical results for performance of the cMLE under the AcAF model with sample sizes 1000, 2000, 5000 and 10000. Mean and S.D. are the sample mean and standard deviation of the cMLE's obtained from 100 simulations.

| Parameter | True value | $N = 1000$ | | $N = 2000$ | | $N = 5000$ | | $N = 10000$ | |
|------------|------------|------------|-------|------------|-------|------------|-------|-------------|-------|
| | | Mean | S.D. | Mean | S.D. | Mean | S.D. | Mean | S.D. |
| γ_0 | 0.230 | 0.269 | 0.167 | 0.248 | 0.154 | 0.234 | 0.119 | 0.213 | 0.091 |
| γ_1 | 0.755 | 0.738 | 0.140 | 0.749 | 0.106 | 0.759 | 0.070 | 0.766 | 0.060 |
| γ_2 | 0.417 | 0.440 | 0.208 | 0.438 | 0.157 | 0.427 | 0.088 | 0.428 | 0.075 |
| γ_3 | 7.114 | 7.507 | 2.805 | 7.589 | 2.706 | 7.385 | 1.939 | 7.083 | 1.737 |
| δ_0 | -0.035 | -0.011 | 0.058 | -0.009 | 0.053 | -0.010 | 0.052 | -0.017 | 0.047 |
| δ_1 | 0.907 | 0.886 | 0.060 | 0.890 | 0.052 | 0.896 | 0.036 | 0.897 | 0.032 |
| δ_2 | 0.425 | 0.475 | 0.183 | 0.446 | 0.133 | 0.436 | 0.083 | 0.435 | 0.068 |
| δ_3 | 4.861 | 5.759 | 2.287 | 5.498 | 1.776 | 5.330 | 1.346 | 5.134 | 1.061 |
| β_0 | -0.244 | -0.227 | 0.090 | -0.236 | 0.063 | -0.234 | 0.042 | -0.235 | 0.032 |
| β_1 | 0.787 | 0.767 | 0.065 | 0.781 | 0.043 | 0.782 | 0.022 | 0.784 | 0.015 |
| β_2 | 0.066 | 0.083 | 0.052 | 0.072 | 0.029 | 0.065 | 0.015 | 0.064 | 0.010 |
| β_3 | 8.111 | 7.348 | 3.555 | 8.097 | 2.845 | 8.216 | 1.968 | 8.107 | 1.586 |
| μ | -0.227 | -0.267 | 0.098 | -0.249 | 0.083 | -0.252 | 0.056 | -0.247 | 0.039 |

5.1 Cross-sectional maxima of the daily negative log-returns of stocks in S&P 500 from high-frequency Bitcoin trading. We note that we model observations from a univariate time series rather than from a bivariate time series even if our model contains four nonlinear time series (in disguise), and decouple the systemic (market) risk into the endopathic and exopathic risks simultaneously. Notice also that the maxima here is equivalent to taking maxima across all stocks' negative log-returns or high-frequency negative log-returns, so we will use these two concepts "maxima" and "maxima of maxima" interchangeably. In all three cases, the AcAF model shows its superiority over the traditional autoregressive tail index models for modeling the endopathic and exopathic competing tail risks in the financial market.

5.1 Cross-sectional maxima of the daily negative log-returns of stocks in S&P 500

In this section, we consider the cross-sectional maxima of the daily negative log-returns (i.e., daily losses) of component stocks in the S&P 500 Index. S&P 500 Index is an American stock market index based on the market capitalizations of 505 large companies, which is among the most commonly followed equity indices and the best representations of the U.S. stock market. To better manage the risk, mutual funds and banks must understand the cross-sectional tail risk of S&P 500. Our data contains the daily clos-

5.1 Cross-sectional maxima of the daily negative log-returns of stocks in S&P 500
ing prices of 505 components of S&P 500 and is downloaded from Yahoo Finance with the time range January 1, 2005, to August 31, 2020.

We present the modeling results for S&P 500 in detail. For each trading day t , we calculate the daily negative log-returns of each component stock in S&P 500 and then calculate the daily cross-sectional maxima $Q_t = \max_{1 \leq i \leq 505} r_{it}$, where r_{it} is the daily negative log-return for stock i . The time series $\{Q_t\}$ contains 3934 observations and is shown in the bottom panel of Figure 1.

The estimation results of our model are summarized in Table 2. From the results we can see: the estimated autoregressive parameter values of $\hat{\gamma}_1$ and $\hat{\delta}_1$ for the tail indices $\{\alpha_{1t}\}$ and $\{\alpha_{2t}\}$ are both close to 1, which suggests a strong persistence of the tail risk processes. The estimated tail indices $\{\hat{\alpha}_{1t}\}$ and $\{\hat{\alpha}_{2t}\}$ are plotted in Figure 1. The range of estimated tail index for endopathic risk is roughly within $[3.26, 10.17]$, while the one for exopathic risk is $[2.68, 29.94]$. Obviously, when the extreme events appear, two tail indices both tend to decrease, reflecting an increase in risk. Moreover, we can see that exopathic risks are more volatile than endopathic risks, especially when extreme events occur. Under normal market conditions, endopathic risks dominate the stock market price fluctuations, while under turbulent market conditions, exopathic risks dominate. This phenomenon

5.1 Cross-sectional maxima of the daily negative log-returns of stocks in S&P 500

shows that α_{1t} and α_{2t} are useful measures of the endopathic and exopathic tail risks, respectively, and our model has a strong ability to capture information of financial crisis, i.e., exopathic risks dominate endopathic risks.

Like what is found in Zhao et al. (2018), the endopathic and exopathic tail indices of S&P 500 experienced sudden downside movement around the end of 2007, which reached their lowest level for the past several years, and the exopathic tail risk index dropped sharply, breaking through the endopathic risk, taking a dominant role. As is said in Zhao et al. (2018), this unusual movement can be viewed as a warning signal of the 2008 financial crisis. Based on Figure 1, we see that the patterns of endopathic risks and exopathic risks can better describe and predict a potential crisis.

A Fréchet type random variable has its k -th moment if and only if $\alpha > k$. It is also noted that all $\hat{\alpha}_{1t}$ and $\hat{\alpha}_{2t}$'s are larger than 2, hence the conditional mean and variance of the cross-sectional maxima always exist, which agrees with the existing literature, e.g., Hansen (1994), and is contrary to some literature findings of the tail index being less than 2 due to a single type of Fréchet distribution specification.

Extending the one-component AcF model (Zhao et al. (2018)) into the two-component AcAF model increases the number of model parameters. In the literature, particularly in models with embedded or hierarchical struc-

5.1 Cross-sectional maxima of the daily negative log-returns of stocks in S&P 500

tures, it is commonly believed that increasing the number of parameters leads to improved performance based on the commonly used performance criteria such as likelihood values, mean squared error (MSE), or prediction mean squared error (PMSE). At first glance, the AcAF model contains more parameters, which, on one hand, leads to better likelihood values. On the other hand, as stated in Remark 7, the key idea of the AcAF model is to find hidden risk factors, i.e., the endopathic and exopathic risks. Our AcAF model's significant contributions are to describe the dynamics of the risk factors. We further note that the new extreme value theory for maxima of maxima guarantees the validity of our proposed model, which can be supported by the findings presented in Table 2 and Figure 1.

There are significant differences between the parameter estimators corresponding to the endopathic and exopathic risks respectively. Note that, for ergodicity, our model setting requires $\gamma_1 \neq \delta_1$ (see Theorem 1). Consider the test for the difference between γ_1 and δ_1 : $H_0 : \gamma_1 = \delta_1$ v.s. $H_1 : \gamma_1 \neq \delta_1$. The test statistic is $\frac{\hat{\gamma}_1 - \hat{\delta}_1}{SD(\hat{\gamma}_1 - \hat{\delta}_1)} = \frac{\hat{\gamma}_1 - \hat{\delta}_1}{\sqrt{var(\hat{\gamma}_1) + var(\hat{\delta}_1) - 2cov(\hat{\gamma}_1, \hat{\delta}_1)}}$. By Table 2 and the covariance obtained from the variance-covariance matrix calculated by Theorem 3, the value of the test statistic is $\frac{0.755 - 0.907}{\sqrt{0.082^2 + 0.006^2 - 2(-0.00012)}} = -1.816$. This shows that although it is difficult to reject H_0 at the 5% significance level, we can reject H_0 at the 10% significance level. Hence we

5.1 Cross-sectional maxima of the daily negative log-returns of stocks in S&P 500

Table 2: Estimated parameters and standard deviations for S&P500 from January 1, 2005 to August 31, 2020.

| | γ_0 | γ_1 | γ_2 | γ_3 | δ_0 | δ_1 | δ_2 | δ_3 |
|-----------|------------|------------|------------|------------|------------|------------|------------|------------|
| Estimates | 0.230 | 0.755 | 0.417 | 7.114 | -0.035 | 0.907 | 0.425 | 4.861 |
| S.D. | 0.149 | 0.082 | 0.148 | 5.007 | 0.064 | 0.006 | 0.003 | 1.445 |
| | β_0 | β_1 | β_2 | β_3 | μ | | | |
| Estimates | -0.244 | 0.787 | 0.066 | 8.111 | -0.227 | | | |
| S.D. | 0.058 | 0.027 | 0.021 | 2.473 | 0.075 | | | |

have enough statistical evidence to support $\gamma_1 \neq \delta_1$.

The estimated scale parameter $\{\hat{\sigma}_t\}$ by our model is shown in Figure 2. For comparison, we also fit a GARCH(1,1) model for each component stock in S&P 500 and plot the daily average volatility given by the GARCH model across the 505 stocks in Figure 2. These two series move very closely with each other, with an overall correlation of 0.65. It suggests that our model's dynamic scale parameter σ_t is an accurate measure of market volatility. Our results are consistent with the ideas in Danielsson and Shin (2003), indicating the stock market is subject to both types of risk. The greatest damage which the stock market are subjected to is done from the risk of the endopathic kind, especially in normal market conditions.

5.2 Intra-day maxima of 5-min negative log-returns of GE stock

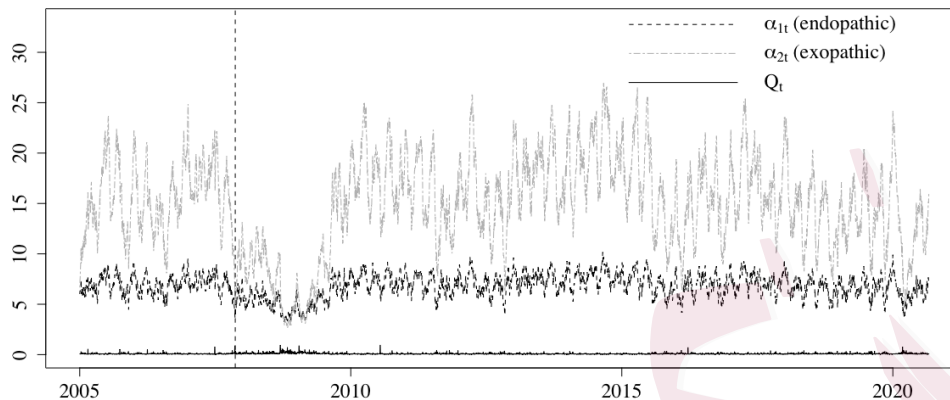


Figure 1: Estimated tail indices $\{\hat{\alpha}_{1t}\}$ and $\{\hat{\alpha}_{2t}\}$, and cross-sectional maximum daily negative log-returns $\{Q_t\}$ of S&P500 Index from January 3, 2005 to August 31, 2020. The sample variances of $\gamma_2 \exp(-\gamma_3 Q_t)$ and $\delta_2 \exp(-\delta_3 Q_t)$ are 0.00591 and 0.00484, respectively.

5.2 Intra-day maxima of 5-min negative log-returns of GE stock

In this section, we consider modeling intra-day maxima of 5-minute negative log-returns of GE stock. We collect the historical 1-minute intra-day GE stock price from January 1, 2008, to June 7, 2013. Then we convert this time series into GE stock prices with time intervals of 5-minute. The 5-minute negative log-returns $\{r_{i,t}\}_{i=1}^p$ are obtained and intra-day maxima Q_t are calculated. The total length of series $\{Q_t\}$ is 1356.

We fit the AcAF model to the intra-day maxima 5-minute negative log-returns series. Estimated parameters and their standard deviations are

5.2 Intra-day maxima of 5-min negative log-returns of GE stock

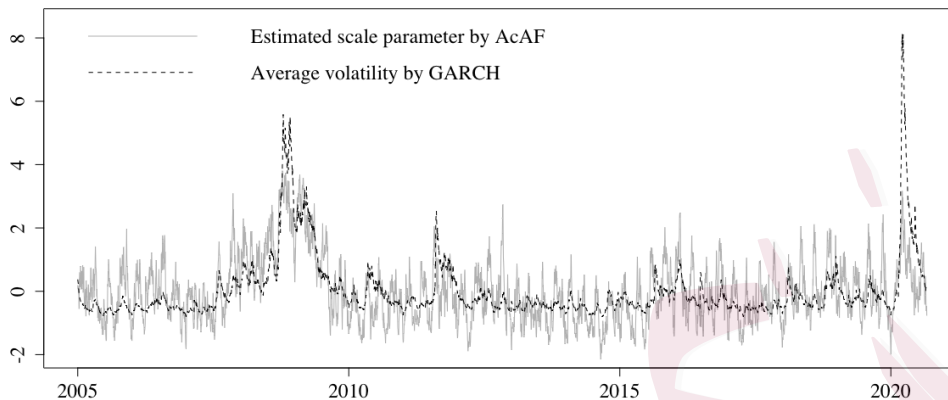


Figure 2: Estimated scale parameter series $\{\hat{\sigma}_t\}$ of S&P500 Index by AcAF model, and estimated average volatility series by GARCH model from January 3, 2005 to August 31, 2020. Both series are standardized to be zero mean and unit variance for comparison.

shown in Table 3. The estimated autoregressive parameters $\hat{\beta}_1$ for $\{\sigma_t\}$ and $\hat{\delta}_1$ for $\{\alpha_{2t}\}$ are close to 1, showing strong persistence of the scale $\{\sigma_t\}$ and exopathic tail risk index $\{\alpha_{2t}\}$ series; while the autoregressive parameter $\hat{\gamma}_1$ for $\{\alpha_{1t}\}$ is 0.303, indicating a less persistence of endopathic tail risk index $\{\alpha_{1t}\}$ series.

The estimated tail indices $\{\hat{\alpha}_{1t}\}$ and $\{\hat{\alpha}_{2t}\}$ are plotted in Figure 3. The range of the estimated tail index for endopathic risk is roughly within $[1.74, 5]$, while the one for exopathic risk is $[1.26, 16.15]$. Obviously, when the extreme events appear, two tail indices both tend to decrease, reflect-

5.2 Intra-day maxima of 5-min negative log-returns of GE stock

Table 3: Estimated parameters and standard deviations for intra-day maxima of 5-minute negative log-returns of GE stock from January 1, 2008 to June 7, 2013.

| | γ_0 | γ_1 | γ_2 | γ_3 | δ_0 | δ_1 | δ_2 | δ_3 |
|-----------|------------|------------|------------|------------|------------|------------|------------|------------|
| Estimates | 0.378 | 0.303 | 0.829 | 81.88 | -0.160 | 0.842 | 0.670 | 41.49 |
| S.D. | 0.384 | 0.306 | 0.331 | 65.51 | 0.106 | 0.024 | 0.016 | 15.32 |
| | β_0 | β_1 | β_2 | β_3 | μ | | | |
| Estimates | -0.240 | 0.939 | 0.063 | 83.30 | -0.007 | | | |
| S.D. | 0.029 | 0.006 | 0.016 | 24.31 | 0.003 | | | |

ing an increase in risk. Moreover, we can see that exopathic risks are more volatile than endopathic risks, especially when extreme values occur. Under normal market conditions, endopathic risks dominate the stock market price fluctuations, while under turbulent market conditions, exopathic risks dominate. This phenomenon is interesting and consistent with the market trading behavior, i.e., the market risks are more dominated by endopathic risks, while the exopathic risks caused by the sentiments of investors can be a driving force of large market variations in high-frequency trading. Figure 3 also shows that on April 14, 2008, the endopathic tail risk index and exopathic tail risk index plummeted, reaching their lowest values since 2008.

5.2 Intra-day maxima of 5-min negative log-returns of GE stock

This can be regarded as an early warning of the financial crisis that began from September 2008. The estimated scale parameter $\{\hat{\sigma}_t\}$ is showed in Figure 5.

From Table 3, we can see that the estimated standard deviations associated with $\hat{\gamma}_0$, $\hat{\gamma}_1$, $\hat{\gamma}_3$ and $\hat{\delta}_0$ are relatively large, and in Figure 3, compared to the estimated $\{\hat{\alpha}_{2t}\}$, the estimated $\{\hat{\alpha}_{1t}\}$ behaves like a constant except during the 2007-2009 financial crisis period. Following Remark 1, we set α_{1t} as static (i.e., in (2.3) we have $\log \alpha_{1t} = \gamma'$), which is a simplified model. Performance of cMLE of the simplified model for intra-day maxima of 5-min negative log-returns of GE stock is shown in Table 4. We can see that all parameters in the simplified model are significant except δ_0 . The estimated $\{\hat{\alpha}_{2t}\}$ together with the constant series $\{\alpha_{1t}\}$ are plotted in Figure 4. We can see that the estimated $\{\hat{\alpha}_{2t}\}$ s in Figures 3 and 4 are very similar, and we calculated their correlation to be 0.9369. From both plots, we see that during normal trading days, the systemic risks faced by large companies such as GE are mainly from internal (endopathic) risks, and during clustered extreme events, e.g., financial crisis, the systemic risks were driven by the exopathic risks.

We note that both the maxima of cross-sectional negative log-returns of stocks from S&P 500 and the maxima of intra-day negative log-returns of

5.2 Intra-day maxima of 5-min negative log-returns of GE stock

Table 4: Estimated parameters and standard deviations of the simplified model for intra-day maxima of 5-minute negative log-returns of GE stock from January 1, 2008 to June 7, 2013.

| | γ' | δ_0 | δ_1 | δ_2 | δ_3 | β_0 | β_1 | β_2 | β_3 | μ |
|-----------|-----------|------------|------------|------------|------------|-----------|-----------|-----------|-----------|--------|
| Estimates | 1.074 | -0.007 | 0.632 | 1.141 | 99.27 | -0.261 | 0.936 | -0.098 | 83.08 | -0.004 |
| S.D. | 0.191 | 0.280 | 0.175 | 0.200 | 39.94 | 0.028 | 0.006 | 0.019 | 20.98 | 0.001 |

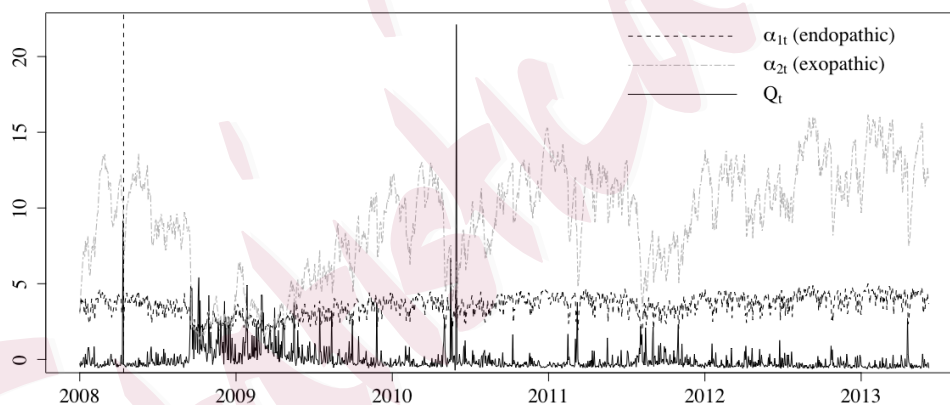


Figure 3: Estimated tail indices $\{\hat{\alpha}_{1t}\}$ and $\{\hat{\alpha}_{2t}\}$, and intra-day maximum of 5-minute negative log-returns $\{Q_t\}$ (normalized) for GE stock from January 1, 2008 to June 7, 2013. The sample variances of $\gamma_2 \exp(-\gamma_3 Q_t)$ and $\delta_2 \exp(-\delta_3 Q_t)$ are 0.03182 and 0.0143, respectively.

5.2 Intra-day maxima of 5-min negative log-returns of GE stock

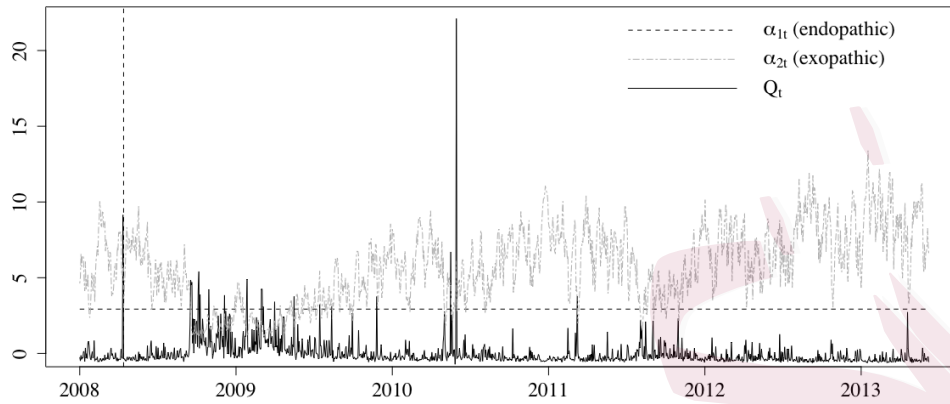


Figure 4: Estimated tail indices $\{\hat{\alpha}_{1t}\}$ and $\{\hat{\alpha}_{2t}\}$, and intra-day maximum of 5-minute negative log-returns $\{Q_t\}$ (normalized) of the simplified model for GE stock from January 1, 2008 to June 7, 2013.

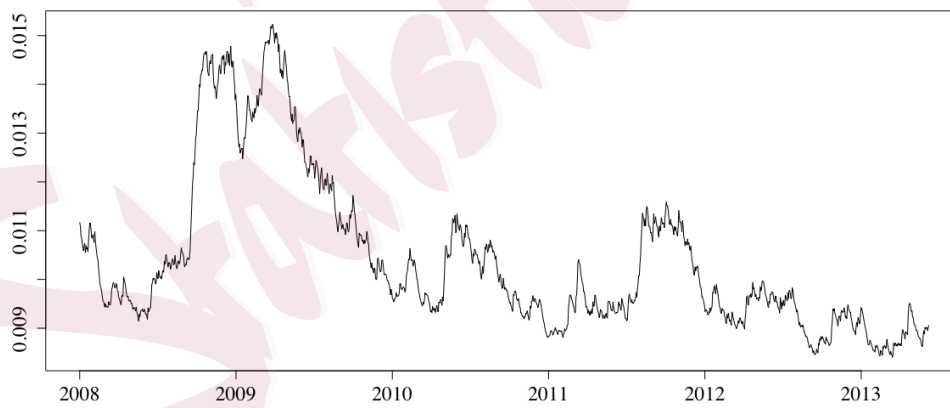


Figure 5: Estimated scale parameter $\{\hat{\sigma}_t\}$ of 5-minute GE stock from January 1, 2008 to June 7, 2013.

5.3 Intra-day maxima of 5-min negative log-returns for BTC/USD exchange rate

high-frequency stock trading lead to similar observations of the 2007-2009 financial crisis. This phenomenon reveals that the AcAF model is robust in describing and predicting market downturn periods.

5.3 Intra-day maxima of 5-min negative log-returns for BTC/USD exchange rate

In this section, we consider modeling intra-day maxima of 5-minute negative log-returns of Bitcoin trading. We convert 1-minute BTC/USD exchange rates to 5-minute frequency time series and obtain daily maxima of negative log-returns Q_t . The exchange rate series we employ is available on Kaggle and includes observations from October 8, 2015, to April 9, 2020. The length of the series $\{Q_t\}$ is 1609.

We fit the model to the intra-day maxima 5-minute negative log-returns series. Estimated parameters and their standard deviations are shown in Table 5. The estimated autoregressive parameters $\hat{\beta}_1$ for $\{\sigma_t\}$ and $\hat{\delta}_1$ for $\{\alpha_{2t}\}$ are close to 1, showing strong persistence of the scale $\{\sigma_t\}$ and exopathic tail risk index $\{\alpha_{2t}\}$ series; while the autoregressive parameter $\hat{\gamma}_1$ for $\{\alpha_{1t}\}$ is 0.416, indicating a less persistence of endopathic tail risk index $\{\alpha_{1t}\}$ series.

The estimated tail indices $\{\hat{\alpha}_{1t}\}$ and $\{\hat{\alpha}_{2t}\}$ are plotted in Figure 6. The

5.3 Intra-day maxima of 5-min negative log-returns for BTC/USD exchange rate

range of estimated tail index for endopathic risk is [2.97, 206.97], while the one for exopathic risk is [5.47, 13.06]. Obviously, when the extreme events appear, two tail indices both tend to decrease, reflecting an increase in risk. Moreover, we can see that endopathic risks are more volatile than exopathic risks, especially when extreme events occur. Exopathic risks dominate the cryptocurrency market price fluctuations under normal market conditions, while under turbulent market conditions, endopathic risks dominate, which is coincident with empirical findings in the literature that policy changes and investor sentiments (exopathic risk) often cause Bitcoin market to suffer very large variations, e.g., Corbet et al. (2014), Dong et al. (2022). The internal transaction risk of the Bitcoin market leads to a large range of price changes, and external shocks have a relatively small impact on Bitcoin trading. However, for the stock market, the risks brought by its internal trading are relatively stable, and the stock price changes are more susceptible to the impact of external shocks.

The estimated scale parameter $\{\hat{\sigma}_t\}$ is showed in Figure 7. Comparing Figures 5 and 7, we see that the scale parameters in maxima of maxima in Bitcoin returns are 5-10 times larger than those in GE stock price changes, which shows a clear pattern that Bitcoin returns are much more volatile than GE returns in terms of high-frequency trading. The competing pat-

5.3 Intra-day maxima of 5-min negative log-returns for BTC/USD exchange rate

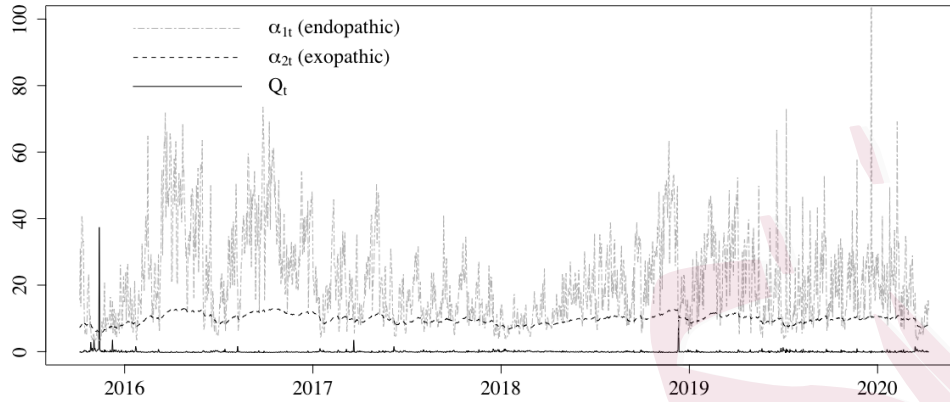


Figure 6: Estimated tail indices $\{\hat{\alpha}_{1t}\}$ and $\{\hat{\alpha}_{2t}\}$, and intra-day maxima of 5-minute negative log-returns $\{Q_t\}$ (normalized) from October 8, 2015 to April 9, 2020 for BTC/USD data. The sample variances of $\gamma_2 \exp(-\gamma_3 Q_t)$ and $\delta_2 \exp(-\delta_3 Q_t)$ are 0.22677 and 0.00051, respectively.

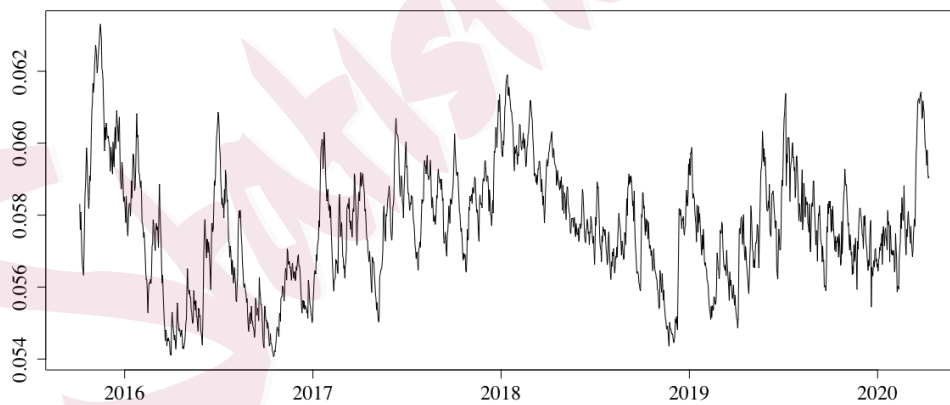


Figure 7: Estimated scale parameter $\{\hat{\sigma}_t\}$ from October 8, 2015 to April 9, 2020 for BTC/USD data.

Table 5: Estimated parameters and standard deviations for intra-day maxima of 5-minute negative log-returns of BTC/USD from October 8, 2015 to April 9, 2020.

| | γ_0 | γ_1 | γ_2 | γ_3 | δ_0 | δ_1 | δ_2 | δ_3 |
|-----------|------------|------------|------------|------------|------------|------------|------------|------------|
| Estimates | 0.598 | 0.416 | 2.004 | 68.57 | 0.100 | 0.920 | 0.118 | 35.195 |
| S.D. | 0.158 | 0.055 | 0.173 | 12.21 | 0.054 | 0.004 | 0.001 | 17.81 |
| | β_0 | β_1 | β_2 | β_3 | μ | | | |
| Estimates | -0.470 | 0.829 | 0.035 | 63.50 | -0.054 | | | |
| S.D. | 0.008 | 0.029 | 0.008 | 15.16 | 0.009 | | | |

terns of the endopathic risks and the exopathic risks from the stock markets are different from those in the Bitcoin markets, i.e., they have reversed relationship.

6. Conclusion

This paper advances the banchmark AcF model to a new autoregressive conditional accelerated Fréchet (AcAF) model for decoupling systemic financial risk into endopathic and exopathic competing risks. Comparatively, this advance is like advancing the ARCH model to the GARCH model in the literature. We model the worst market returns using maxima of maxima

in financial time series, which provides a new angle to identify systemic risk patterns and their impacts in financial markets. The probabilistic properties of stationarity and ergodicity of the AcAF model are investigated. We implement the cMLE for the AcAF model, and the estimators' consistency and asymptotic properties are established. The proof extends the theoretical result to a dynamic model for nonlinear time series driven by two variables. Simulation study shows the AcAF model's superior performance to the existing dynamic GEV models for heterogeneous data and the efficiency of the proposed estimators. The real data examples illustrate its potential broad use in financial risk management and systemic risk monitoring. It provides a clear risk pattern of market risks and the causes of the financial crisis.

The AcAF model can be extended to many other aspects. One potential extension is to assume a dynamic structure for the location parameter μ . Another future direction is to extend two risk sources to multiple sources of risk with the construction of a flexible multivariate dynamic tail risk model.

The AcAF model can be applied to diversified areas as long as decoupling systemic risks into competing endopathic risks and exopathic risks is concerned. These areas include systemic risks in social, political, economic, financial, market, regional, global, environmental, transportation,

epidemiological, material, chemical, and physical systems.

Supplementary material

Supplementary material for “Decoupling Systemic Risk into Endopathic and Exopathic Competing Risks Through Autoregressive Conditional Accelerated Fréchet Model” contains proofs of Theorem 1, Proposition 1, Theorems 2 and 3, and Proposition 2, along with the auxiliary lemmas, and the expressions of the first order and the second order partial derivatives of the likelihood function in the paper, as well as three more simulation studies.

Acknowledgments

The authors thank the editor, associate editor, and reviewers for their valuable comments and suggestions. We thank the seminar participants at the 2021 NBER-NSF Time Series Conference, the 2021 Extreme Value Analysis Conference, the 2021 Symposium on Modern Statistics, and the 2021 academic lecture of Shandong Big Data and Finance Research Association. Jingyu Ji’s research was partially supported by the National Natural Science Foundation of China grants 71991471 when she was a PhD student at Fudan University. Deyuan Li’s research was partially supported by the National Natural Science Foundation of China grants 11971115. Zhengjun

REFERENCES

Zhang's research was partially supported by the National Natural Science Foundation of China grants 71991471 and NSF-DMS-2012298.

References

Bali, T. G. and D. Weinbaum (2007). A conditional extreme value volatility estimator based on high-frequency returns. *Journal of Economic Dynamics and Control* 31(2), 361–397.

Bollerslev, T. (1986). Generalized autoregressive conditional heteroskedasticity. *Journal of Econometrics* 31(3), 307–327.

Cao, W. and Z. Zhang (2021). New extreme value theory for maxima of maxima. *Statistical Theory and Related Fields* 5(3), 232–252.

Chavez-Demoulin, V., P. Embrechts, and M. Hofert (2016). An extreme value approach for modeling operational risk losses depending on covariates. *Journal of Risk and Insurance* 83(3), 735–776.

Chavez-Demoulin, V., P. Embrechts, and S. Sardy (2014). Extreme-quantile tracking for financial time series. *Journal of Econometrics* 181(1), 44–52.

Corbet, S., G. McHugh, and A. Meegan (2014). The influence of central bank monetary policy announcements on cryptocurrency return volatility. *Investment Management and Financial Innovations* 14(4), 60–72.

REFERENCES

- Danielsson, J. and H. S. Shin (2003). Endogenous risk. In *Modern Risk Management: A History*, pp. 297–316. Risk Books.
- Daouia, A., S. Girard, and G. Stupfler (2018). Estimation of tail risk based on extreme expectiles. *Journal of the Royal Statistical Society: Series B (Statistical Methodology)* 80(2), 263–292.
- Deng, L., M. Yu, and Z. Zhang (2020). Statistical learning of the worst regional smog extremes with dynamic conditional modeling. *Atmosphere* 11(6), 665. doi:10.3390/atmos11060665.
- Dong, F., Z. Xu, and Y. Zhang (2022). Bubbly bitcoin. *Economic Theory* 74, 973–1015.
- Embrechts, P., S. I. Resnick, and G. Samorodnitsky (1999). Extreme value theory as a risk management tool. *North American Actuarial Journal* 3(2), 30–41.
- Engle, R. F. and J. R. Russell (1998). Autoregressive conditional duration: a new model for irregularly spaced transaction data. *Econometrica* 66(5), 1127–1162.
- Farboodi, M., G. Jarosch, and R. Shimer (2021). Internal and external ef-

REFERENCES

- fects of social distancing in a pandemic. *Journal of Economic Theory* 196, 105293.
- Hansen, B. E. (1994). Autoregressive conditional density estimation. *International Economic Review* 35(3), 705–730.
- Harvey, A. C. (2013). *Dynamic Models for Volatility and Heavy Tails: with Applications to Financial and Economic Time Series*, Volume 52. Cambridge University Press.
- Heffernan, J. E., J. A. Tawn, and Z. Zhang (2007). Asymptotically (in)dependent multivariate maxima of moving maxima processes. *Extremes* 10, 57–82.
- Idowu, T. and Z. Zhang (2017). An extended sparse max-linear moving model with application to high-frequency financial data. *Statistical Theory and Related Fields* 1(1), 92–111.
- Ji, J. and D. Li (2021). Application of autoregressive tail-index model to China’s stock market. *Statistical Theory and Related Fields* 5(1), 31–34.
- Kelly, B. and H. Jiang (2014). Tail risk and asset prices. *Review of Financial Studies* 27(10), 2841–2871.
- Koo, C. K., A. Semeyutin, C. Lau, and J. Fu (2020). An application of

REFERENCES

- autoregressive extreme value theory to cryptocurrencies. *The Singapore Economic Review*, 1–8. doi:10.1142/S0217590820470013.
- Leadbetter, M. R., G. Lindgren, and H. Rootzén (1983). *Extremes and Related Properties of Random Sequences and Processes*. Springer Science & Business Media.
- Lopez, J. A. and M. R. Saldenbergh (2000). Evaluating credit risk models. *Journal of Banking & Finance* 24(1-2), 151–165.
- Malinowski, A., M. Schlather, and Z. Zhang (2015). Marked point process adjusted tail dependence analysis for high-frequency financial data. *Statistics and Its Interface* 8(1), 109–122.
- Mao, G. and Z. Zhang (2018). Stochastic tail index model for high frequency financial data with bayesian analysis. *Journal of Econometrics* 205(2), 470–487.
- Massacci, D. (2017). Tail risk dynamics in stock returns: Links to the macroeconomy and global markets connectedness. *Management Science* 63(9), 3072–3089.
- McNeil, A. J. and R. Frey (2000). Estimation of tail-related risk measures

REFERENCES

- for heteroscedastic financial time series: an extreme value approach. *Journal of Empirical Finance* 7(3-4), 271–300.
- Naveau, P., Z. Zhang, and B. Zhu (2011). An extension of max autoregressive models. *Statistics and its Interface* 4(2), 253–266.
- Poon, S.-H., M. Rockinger, and J. Tawn (2004). Extreme value dependence in financial markets: Diagnostics, models, and financial implications. *The Review of Financial Studies* 17(2), 581–610.
- Smith, R. L. and D. Goodman (2000). Bayesian risk analysis. In *Extremes and Integrated Risk Management*, Chapter 17. Risk Books.
- Tang, R., J. Shao, and Z. Zhang (2013). Sparse moving maxima models for tail dependence in multivariate financial time series. *Journal of Statistical Planning and Inference* 143(5), 882–895.
- Zhang, Z. (2021a). On studying extreme values and systematic risks with nonlinear time series models and tail dependence measures. *Statistical Theory and Related Fields* 5(1), 1–25.
- Zhang, Z. (2021b). Rejoinder of “on studying extreme values and systematic risks with nonlinear time series models and tail dependence measures”. *Statistical Theory and Related Fields* 5(1), 45–48.

REFERENCES

Zhang, Z. and R. L. Smith (2010). On the estimation and application of max-stable processes. *Journal of Statistical Planning and Inference* 140(5), 1135–1153.

Zhang, Z. and B. Zhu (2016). Copula structured M4 processes with application to high-frequency financial data. *Journal of Econometrics* 194(2), 231–241.

Zhao, Z., Z. Zhang, and R. Chen (2018). Modeling maxima with autoregressive conditional Fréchet model. *Journal of Econometrics* 207(2), 325–351.

Jingyu Ji

School of Statistics, Capital University of Economics and Business, Beijing, China

E-mail: jingyuji@cueb.edu.cn

Deyuan Li (Corresponding author)

School of Management, Fudan University, Shanghai, China

E-mail: deyuanli@fudan.edu.cn

Zhengjun Zhang (Corresponding author)

School of Economics and Management, and MOE Social Science Laboratory

REFERENCES

of Digital Economic Forecasts and Policy Simulation, University of Chinese

Academy of Sciences, Beijing, China;

Center for Forecasting Sciences, Chinese Academy of Sciences, Beijing,

China;

Department of Statistics, University of Wisconsin, Madison, WI, USA

E-mail: zhangzhengjun@ucas.ac.cn